Control Oriented Modular Modelling of a Floating Wind Turbine: The Port-Hamiltonian Approach ⋆

Ignacio Diaz * **Yann LeGorrec** * **Yongxin Wu** *

* *Université Marie et Louis Pasteur, SUPMICROTECH, CNRS, institut FEMTO-ST, F-25000, Besançon, France,(emails: ignacio.diaz@femto-st.fr, yann.le.gorrec@femto-st.fr, yongxin.wu@femto-st.fr).*

Abstract: This paper proposes a control-oriented model of a floating wind turbine, incorporating 2D platform motion via a coupled beam-string structure with axial and transversal deformations. The model of the floating turbine includes the rigid body rotations of the floating platform, maintaining the small deformation approximation for the beam. The port-Hamiltonian approach is used for its modularity and to reflect the system's passivity. Simulations using a simplified water-structure interaction modelled by Archimedes' forces on a rectangular platform are given. Leveraging system modularity, control alternatives are discussed.

Keywords: Floating systems, flexible structures, port Hamiltonian systems.

1. INTRODUCTION

The offshore wind industry is one of the fastest-growing renewable energy sectors. Thus, designing reliable and cost-efficient offshore energy generation systems is therefore of crucial interest, leading to increased research into the modelling and simulation of these complex systems (Robertson et al., 2014). One of the offshore wind energy conversion systems is the floating wind turbine (FWT) which includes a wind generator tower, a floating platform, and a mooring system that allows access to deep waters (Cruz and Atcheson, 2016). The different aerodynamic and hydrodynamic interactions with the structure can lead to undesired behaviours, such as vibrations or external disturbances leading to unreliability in the structure and therefore requiring structural analysis and control design (He et al., 2020). Some of the previously discussed control strategies for FWT have been designed with rigid body models (Bakka et al., 2014), tuned through simulation softwares like FAST (Salic et al., 2019) or developed using input-output linear models derived from time response data (Li and Gao, 2016). In He et al. (2020), a simple distributed parameter model with horizontal (small) deformations and displacements was proposed and used to design a vibration reduction control strategy.

In this paper, we propose an extended distributed parameter model with horizontal and vertical displacements and deformations, combined with a rigid body rotation. The purpose of this extension is to capture the effects of buoyancy and gravity more precisely. This leads to a model represented by a larger set of partial differential equations (PDEs) combined with ordinary differential equations (ODEs). One tool that has been useful for the analysis and control of such systems is the port-Hamiltonian (PH) framework, a modelling paradigm based on power-preserving structures (Maschke and van der Schaft, 2000). The advantage of using the PH framework lies in its structure that reflects the passivity of the systems and its modularity, leading to strong results in analysis (Le Gorrec et al., 2005), control (Rodriguez et al., 2001), and discretisation (Golo et al., 2004).

The following section describes the system under consideration and how it can be decomposed into subsystems. This section also provides some notations and main assumptions. In Section 3 the Hamilton's principle is used to derive each of the subsystem's dynamic equations. The following section presents some simulation results and discusses some control perspectives. The paper end with some concluding remarks and perspectives.

2. PROPOSED SYSTEM

The system under consideration is depicted in Figure 1. It is composed of four subsystems, namely the Mooring lines, the Floating Wind Turbine Beam, the Floating Platform and the Nacelle, Rotor and Blades (NRB). In this section are given the main assumptions made for each of these subsystems. These assumption are associated to a motion of the system in a two dimensional space including rigid body rotations for the FWT beam.

2.1 Notation

For the flexible bodies, Ω is the domain in the local coordinates. When a sub-index appears, it refers to the independent coordinates and the fixed coordinates are received as input. As an example $\Omega_{23}(\bar{\xi}_1)$ represents the section of the body in the $\Xi_2 \times \Xi_3$ plan that passes by

⋆ This project has received funding from the European Union's Horizon Europe research and innovative programme under the Marie Skłodowska-Curie Actions (MSCA) grant agreement No. 101073558 (ModConFlex).

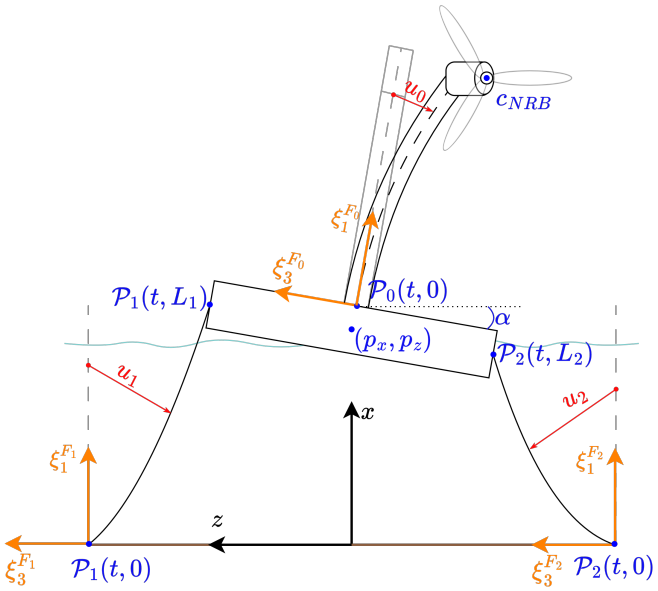

Fig. 1. Proposed Model Diagram

$\bar{\xi_1}$, i.e. the points $(\bar{\xi_1}, \xi_2, \xi_3) \in \Omega$. While Ω_1 represents the domain of ξ_1 that passes $\xi_2 = \xi_3 = 0$.

2.2 Mooring Lines

The mooring lines of the floating wind turbine are modelled using flexible strings with axial and transversal deformations. The transversal section remains constant through the deformation and depends only on the local coordinate along the neutral axis. Considering that the local coordinates F_i of the i-th mooring line is described by $\xi^{F_i} = \left(\xi_1^{F_i} \ \xi_2^{F_i} \ \xi_3^{F_i}\right)^T$, the assumption on the section can be expressed as

$$A_i(\xi_1^{F_i}) = \iint_{\Omega_{23}^{F_i}(\xi_1^{F_i})} dA. \tag{1}$$

Additionally, the position of an arbitrary point in the mooring line given the proposed assumptions can be described as

$$\mathcal{P}_i(t, \xi^{F_i}) = c_i + \left(\xi^{F_i} + u_i(t)\right), \tag{2}$$

where

$$c_i = \begin{pmatrix} 0 \\ 0 \\ z_i \end{pmatrix}, \quad \xi^{F_i} = \begin{pmatrix} \xi_1^{F_i} \\ \xi_2^{F_i} \\ \xi_3^{F_i} \end{pmatrix} \quad \text{and} \quad u_i = \begin{pmatrix} v_i(t, \xi_1^{F_i}) \\ 0 \\ w_i(t, \xi_1^{F_i}) \end{pmatrix},$$

where $v_i(t, \cdot)$ and $w_i(t, \cdot)$ are at least C^2 in Ω^{F_i}.

Finally, the following considerations are taken into account for the interconnection:

- The mooring line is fixed at the bottom at point
$$\mathcal{P}_i(t, 0_{3\times 1}) = c_i. \tag{3}$$
- The mooring line is fixed at the top at point
$$\mathcal{P}_i\left(t, \begin{pmatrix} L_i \\ 0 \\ 0 \end{pmatrix}\right) = \begin{pmatrix} p_x(t) + (-1)^{1+i}\frac{L}{2}\sin\alpha(t) \\ 0 \\ p_z(t) + (-1)^{1+i}\frac{L}{2}\cos\alpha(t) \end{pmatrix}, \tag{4}$$
given by the position $\left(p_x(t), 0, p_z(t)\right)$ and angle $\alpha(t)$ of the floating platform.

2.3 Floating Wind Turbine Beam

The FWT beam is modelled as an extension of a Timoshenko beam. In this extension, we consider both transversal deformation of the neutral axis and axial deformation. The section of the beam remains constant through the deformation but remains orthogonal to the neutral axis. An additional rigid body rotation α is considered. Considering the local coordinates F_0 of the beam described by $\xi^{F_0} = \left(\xi_1^{F_0} \ \xi_2^{F_0} \ \xi_3^{F_0}\right)^T$, the supposition that the area of the transversal section remains constant can be expressed as (1) with $i = 0$. Finally, the base of the FWT depends on the position of the floating platform, with this, the position of an arbitrary point in the beam given the proposed assumptions can be described as

$$\mathcal{P}_0(t, \xi^{F_0}) = c_0(t) + R_\alpha(t)\left(\xi^{F_0} + u_0(t)\right), \tag{5}$$

where

$$c_0(t) = \begin{pmatrix} p_x(t) + \frac{h}{2}\cos\left(\alpha(t)\right) \\ 0 \\ p_z(t) - \frac{h}{2}\sin\left(\alpha(t)\right) \end{pmatrix}, \quad \xi^{F_0} = \begin{pmatrix} \xi_1^{F_0} \\ \xi_2^{F_0} \\ \xi_3^{F_0} \end{pmatrix},$$

$$u_0(t) = \begin{pmatrix} v_0(t, \xi_1^{F_0}) - \xi_3^{F_0}\sin\left(\phi(t, \xi_1^{F_0})\right) \\ 0 \\ w_0(t, \xi_1^{F_0}) - \xi_3^{F_0}\left(1 - \cos\left(\phi(t, \xi_1^{F_0})\right)\right) \end{pmatrix},$$

and

$$R_\alpha(t) = \begin{pmatrix} \cos\left(\alpha(t)\right) & 0 & \sin\left(\alpha(t)\right) \\ 0 & 1 & 0 \\ -\sin\left(\alpha(t)\right) & 0 & \cos\left(\alpha(t)\right) \end{pmatrix},$$

where $v_0(t, \cdot)$, $w_0(t, \cdot)$ and $\phi(t, \cdot)$ are at least C^2 in Ω^{F_0}. $p_x(t)$, $p_z(t)$ and $\alpha(t)$ are given by the position of the floating platform and $\frac{h}{2}$ is the distance between the centre of mass of the floating platform and the base of the beam.

Finally, the following considerations are taken into account for the interconnection:

- The mooring line is fixed at the bottom at point
$$\mathcal{P}_0\left(t, 0_{3\times 1}\right) = \begin{pmatrix} p_x(t) + \frac{h}{2}\cos\alpha \\ 0 \\ p_z(t) - \frac{h}{2}\sin\alpha \end{pmatrix}, \tag{6}$$
given by the position $\left(p_x(t), 0, p_z(t)\right)$ and angle $\alpha(t)$ of the floating platform.
- The mooring line is fixed at the top at point
$$\mathcal{P}_0\left(t, (L_0 \ \ 0 \ \ 0)^T\right) = c_{NRB}(t), \tag{7}$$
which corresponds to the position of the lumped nacelle, rotor and blades system.

2.4 Floating Platform

In this paper the floating platform is modelled by a lumped system, this consideration is done to simplify the water-structure interactions. For this paper, the fluid structure interactions are modelled using only the Archimedes forces, avoiding water dynamics and terms like the added mass effect (Lannes, 2017). For the remaining of this paper, we consider that the floating platform can be approximated to a rectangular body of height h and length L. With this in mind, the calculations of the Archimedes forces and torques can be found in the Appendix A.

2.5 Nacelle, Rotor and Blades

Finally, the other lumped system considers the nacelle rotor and blades effect. This is approximated as a lumped mass at the tip of the beam and a rotating inertia for the rotation of the section. This inertia is mainly given by the blades and can be approximated as

$$I_\ell^2 = k_J M_\ell^2 {L_B}^2, \tag{8}$$

where M_ℓ^2 is the mass of the lumped NRB, L_B is the length of the blades and k_J is a factor due to geometry described in González Rodriguez et al. (2007).

3. MODULAR SYSTEM MODELLING

This section presents the energy variables, the Hamiltonian, port-Hamiltonian formulation and the respective input/output of each subsystem.

3.1 Mooring Lines

Following the undeformed section area given by (1) and the displacement given by (2), the momentum of an arbitrary point in the mooring line is given by

$$p_i(t) = \begin{pmatrix} A_i\rho_i\dot{v}_i(t) & 0 & A_i\rho_i\dot{w}_i(t) \end{pmatrix}^T, \tag{9}$$

where $\dot{f}(t) = \frac{\partial f(t)}{\partial t}$, and ρ_i may be a function of $\xi_1^{F_i}$. With this, the kinetic energy can be expressed as

$$K_i(t) = \frac{1}{2}\int_{\Omega_1^{F_i}} p_i^T M_i p_i d\xi_1^{F_i}, \tag{10}$$

where

$$M_i(\xi_1^{F_i}) = \begin{pmatrix} 1 & 0 & 0 \\ 0 & 0 & 0 \\ 0 & 0 & 1 \end{pmatrix} \frac{1}{(A_i\rho_i)}.$$

To obtain the elastic potential energy due to the deformation of the string, the small deformation approximation is considered. Therefore the strain is given by the symmetric gradient operator

$$\mathrm{Grad}(u) = \frac{1}{2}(\nabla u + \nabla u^T). \tag{11}$$

In Voigt-Kelvin (VK) notation, the strain tensor can be expressed as a vector following the structure

$$\epsilon^i = (\epsilon_1^i \;\; \epsilon_2^i \;\; \epsilon_3^i \;\; 2\epsilon_{23}^i \;\; 2\epsilon_{13}^i \;\; 2\epsilon_{12}^i)^T,$$

thus the strain of the mooring line model can be expressed as

$$\epsilon^i(t, \xi_1^{F_i}) = \begin{pmatrix} v_i'(t) \\ 0 \\ 0 \\ 0 \\ w_i'(t) \\ 0 \end{pmatrix}, \tag{12}$$

where $f'(\xi_1^{F_i}) = \frac{\partial f(\xi_1^{F_i})}{\partial \xi_1^{F_i}}$. The elastic potential energy of the mooring line can be then expressed as

$$U_i(t) = \frac{1}{2}\int_{\Omega_1^{F_i}} (\epsilon^i)^T C_i \epsilon^i d\xi_1^{F_i}, \tag{13}$$

where

$$C_i(\xi_1^{F_i}) = \mathrm{diag}\Big[\, (E_iA_i \;\; 0 \;\; 0 \;\; 0 \;\; G_iA_i \;\; 0) \,\Big].$$

As a consequence, it is possible to express the mooring line model as a PHS, where the Hamiltonian is the sum of (10) and (13). The energy variables are given by (9) and (12)

$$\zeta^i = \begin{pmatrix} v_i' & w_i' & A_i\rho_i\dot{v}_i & A_i\rho_i\dot{v}_i 1 \end{pmatrix}^T, \tag{14}$$

and the Hamiltonian can be expressed as

$$H_i(t) = \frac{1}{2}\int_{\Omega_1^{F_i}} (\zeta^i)^T \mathcal{H}_i \zeta^i d\xi_1^{F_i}, \tag{15}$$

and the energy density is modulated by

$$\mathcal{H}_i = \mathrm{diag}\begin{pmatrix} E_iA_i & G_iA_i & \frac{1}{A_i\rho_i} & \frac{1}{A_i\rho_i} \end{pmatrix}. \tag{16}$$

The dynamic equations for ζ^i are derived from Hamilton's principle as presented in (Ponce et al., 2024), leading to the following PDE

$$\dot{\zeta}^i = P_1^i \frac{\partial}{\partial \xi_1^{F_i}}\big(\mathcal{H}_i\zeta^i\big), \tag{17}$$

where

$$P_1^i = \begin{pmatrix} 0_2 & I_2 \\ I_2 & 0_2 \end{pmatrix}. \tag{18}$$

Thus, the boundary efforts and flows can be parametrized as presented in (Le Gorrec et al., 2005) by

$$\begin{pmatrix} f_\partial^i \\ e_\partial^i \end{pmatrix} = \frac{1}{\sqrt{2}}\begin{pmatrix} P_1^i & -P_1^i \\ I_4 & I_4 \end{pmatrix}\begin{pmatrix} \mathcal{H}_i\zeta^i\big|_{L_i} \\ \mathcal{H}_i\zeta^i\big|_0 \end{pmatrix}, \tag{19}$$

where P_1^i is defined by (18). Finally, from (3) and (4) the boundary inputs at $\xi_1^{F_i} = 0$ and $\xi_1^{F_i} = L_i$ are velocity inputs, because they are imposed by the external system. Then inputs and outputs can be formulated as a combination of the boundary variables as

$$u_\partial^i = W_B^i \begin{pmatrix} f_\partial^i \\ e_\partial^i \end{pmatrix} \qquad y_\partial^i = W_C^i \begin{pmatrix} f_\partial^i \\ e_\partial^i \end{pmatrix}, \tag{20}$$

where

$$W_B^i = \frac{1}{\sqrt{2}}\begin{pmatrix} -I_2 & 0_2 & 0_2 & I_2 \\ I_2 & 0_2 & 0_2 & I_2 \end{pmatrix} \quad W_C^i = \frac{1}{\sqrt{2}}\begin{pmatrix} 0_2 & I_2 & -I_2 & 0_2 \\ 0_2 & I_2 & I_2 & 0_2 \end{pmatrix}.$$

This leads to the energy balance

$$\dot{H}_i = {u_\partial^i}^T y_\partial^i.$$

3.2 Floating Wind Turbine Beam

Following the undeformed section area approximation given by (1), with $i = 0$ and the displacement given by (5), the generalized momentum of an arbitrary point in the wind turbine beam using linear and angular momenta is given by

$$p_0(t) = \begin{pmatrix} A_0\rho_0 v_a(t) & A_0\rho_0 v_t(t) & I_0\rho_0 r(t) \end{pmatrix}^T, \tag{21}$$

where v_a, v_t and r are the axial velocity, tangential velocity and angular velocity of the section defined by

$$\begin{aligned} v_a(t, \xi_1^{F_0}) =& \dot{\alpha}(t) w_0(t, \xi_1^{F_0}) + \dot{v}_0(t, \xi_1^{F_0}) + \dots \\ & \cdots + \dot{p}_x(t)\cos\big(\alpha(t)\big) - \dot{p}_z(t)\sin\big(\alpha(t)\big), \end{aligned} \tag{22}$$

$$\begin{aligned} v_T(t, \xi_1^{F_0}) =& -\dot{\alpha}(t)\Big(\xi_1^{F_0} + v_0(t, \xi_1^{F_0}) + \frac{h}{2}\Big) + \dots \\ & \cdots + \dot{w}_0(t, \xi_1^{F_0}) + \dot{p}_x(t)\sin\big(\alpha(t)\big) + \dots \\ & \cdots + \dot{p}_z(t)\cos\big(\alpha(t)\big), \end{aligned} \tag{23}$$

$$r(t, \xi_1^{F_0}) = \dot{\phi}(t, \xi_1^{F_0}) - \dot{\alpha}(t), \tag{24}$$

I_0 is the rotational inertia of the section defined by

$$I_0(\xi_1^{F_0}) = \iint_{\Omega_{23}^{F_0}(\xi_1^{F_0})} {\xi_3}^2 dA, \tag{25}$$

and ρ_0 may be a function of $\xi_1^{F_0}$.

The kinetic energy can be expressed as (10), with $i = 0$, and where

$$M_0(\xi_1^{F_0}) = \begin{pmatrix} 1 & 0 & 0 \\ 0 & 1 & 0 \\ 0 & 0 & 0 \end{pmatrix} \frac{1}{A_0\rho_0} + \begin{pmatrix} 0 & 0 & 0 \\ 0 & 0 & 0 \\ 0 & 0 & 1 \end{pmatrix} \frac{1}{I_0\rho_0}. \tag{26}$$

To obtain the elastic potential energy due to the deformation of the beam, the small deformation approximation is considered just like in the string case. We then consider the strain as in (11) and the quadratic energy density described by the generalized Hooke's law. This energy can be then expressed using the generalized displacement vector given by

$$\epsilon^0(t, \xi_1^{F_0}) = \begin{pmatrix} v_0'(t) & w_0'(t) - \phi(t) & \phi'(t) \end{pmatrix}^T, \tag{27}$$

obtaining the elastic potential energy as in (13) with $i = 0$, and where

$$C_0(\xi_1^{F_0}) = \text{diag}\Big[\begin{pmatrix} E_0A_0 & G_0A_0 & E_0I_0 \end{pmatrix} \Big]. \tag{28}$$

As a result, it is possible to express the FWT as a PHS, where the Hamiltonian is the sum of (10) and (13), with $i = 0$, by using the previous definitions (21), (26), (27) and (28). The energy variables are given by (21) and (27)

$$\zeta^0 = \begin{pmatrix} v_0' & w_0' - \phi & \phi' & A_0\rho_0 v_a & A_0\rho_0 v_t & I_0\rho_0 r \end{pmatrix}, \tag{29}$$

and the Hamiltonian can be expressed as in (15) with $i = 0$ and the energy density is modulated by

$$\mathcal{H}_0 = \text{diag}\left(E_0A_0 \;\; G_0A_0 \;\; E_0I_0 \;\; \frac{1}{A_0\rho_0} \;\; \frac{1}{A_0\rho_0} \;\; \frac{1}{I_0\rho_0} \right). \tag{30}$$

It is then possible to obtain dynamic equations for ζ^0 from Hamilton's principle, leading to the following PDE

$$\dot{\zeta}^0 = \left(P_1^0 \frac{\partial(\cdot)}{\partial \xi_1^{F_0}} + P_0^0 \right) \mathcal{H}_0 \zeta^0 + B_R u_R, \tag{31}$$

where

$$\begin{gathered} P_1^0 = \begin{pmatrix} 0_3 & I_3 \\ I_3 & 0_3 \end{pmatrix}, \quad P_0^0 = \begin{pmatrix} 0_3 & M_0^0 \\ -{M_0^0}^T & 0_3 \end{pmatrix}, \\ M_0^0 = \begin{pmatrix} 0 & 0 & 0 \\ 0 & 0 & -1 \\ 0 & 0 & 0 \end{pmatrix}, \end{gathered} \tag{32}$$

and the pair B_R, u_R represents the distributed forces and velocities that have to be considered for the beam to obtain a rigid body rotation. They are described by

$$\begin{gathered} B_R = \begin{pmatrix} f(\zeta^0) & \zeta_4^0 & 0 & -\zeta_2^0 & \zeta_1^0 & 0 \\ 1 & 0 & 0 & 0 & 0 & 0 \end{pmatrix}^T, \; u_R = \begin{pmatrix} \dot{\alpha} \\ \alpha\dot{\alpha} \end{pmatrix}, \\ f(\zeta^0) = -\zeta_5^0 + \int_0^{\xi_1^{F_0}} \zeta_6^0(t, \xi) d\xi. \end{gathered} \tag{33}$$

With a distributed input port it is necessary to define the conjugated output which is given by

$$y_R = \int_0^{L_0} {B_R}^T \mathcal{H}_0 \zeta^0 d\xi_1^{F_0}. \tag{34}$$

Similarly to what was done for the mooring line system, the boundary efforts and flows can be parametrized by (19) with $i = 0$. Finally, from (6) and (7) the boundary inputs at $\xi_1^{F_0} = 0$ and $\xi_1^{F_0} = L_0$ are velocity inputs, because they are imposed by external systems. Thus the inputs and outputs of the system can be derived as a combination of the boundary variables given by (20), i.e.

$$W_B^0 = \frac{1}{\sqrt{2}} \begin{pmatrix} -I_3 & 0_3 & 0_3 & I_3 \\ I_3 & 0_3 & 0_3 & I_3 \end{pmatrix} \quad W_C^0 = \frac{1}{\sqrt{2}} \begin{pmatrix} 0_3 & I_3 & -I_3 & 0_3 \\ 0_3 & I_3 & I_3 & 0_3 \end{pmatrix}.$$

This leads to the following energy balance

$$\dot{H}_0 = {u_\partial^0}^T y_\partial^0$$

3.3 Floating Platform

The floating platform is approximated by a lumped system with fluid structure interactions, which are conservative and given by the Archimedes forces. Thus, the energy of the system is composed of the kinetic energy as a function of the generalized displacement variables $\dot{p}_x$, $\dot{p}_z$, and $\dot{\alpha}$ and the non-linear potential energy defined by p_x and the angle α. This non-linear potential energy must fulfill the following relations

$$\frac{\partial U_W^{\ell 1}}{p_x} = -F_W, \qquad \frac{\partial U_W^{\ell 1}}{\alpha} = \tau_W, \tag{35}$$

where F_W and τ_W are the forces and torques calculated in Appendix A. By choosing the energy variables as

$$\mathrm{x}^1 = \begin{pmatrix} p_x & \alpha & M_1^\ell \dot{p}_x & M_1^\ell \dot{p}_z & I_1^\ell \dot{\alpha} \end{pmatrix}^T, \tag{36}$$

the Hamiltonian can be written

$$H_1^\ell(\mathrm{x}^1) = \frac{1}{2}(x^1)^T \mathcal{H}_1^\ell x^1 + U_W^{\ell 1}, \tag{37}$$

where

$$\mathcal{H}_1^\ell = \begin{pmatrix} 0_2 & 0_{2\times 3} \\ 0_{3\times 2} & \text{diag}\begin{pmatrix} M_1^\ell & M_1^\ell & I_1^\ell \end{pmatrix}^{-1} \end{pmatrix}. \tag{38}$$

From this definition of the Hamiltonian, it is possible to derive the dynamic equations for x^1 using the Hamilton's principle. In this step it is important to take into consideration the interaction with each distributed systems adjusted to the local reference frame using energy preserving interconnections. This leads to the following ODEs

$$\dot{\mathrm{x}}^1 = J \frac{\partial H_1^\ell}{\partial \mathrm{x}^1} + B_{1R_\alpha}^\ell u_{1R_\alpha}^\ell + \sum_{i=1}^{2} B_{XZ}^i u_{XZ}^i + B_d^\ell u_d^\ell + u_C^{1\ell}, \tag{39}$$

where

$$\begin{gathered} J = \begin{pmatrix} 0 & 0 & 1 & 0 & 0 \\ 0 & 0 & 0 & 0 & 1 \\ -1 & 0 & 0 & 0 & 0 \\ 0 & 0 & 0 & 0 & 0 \\ 0 & -1 & 0 & 0 & 0 \end{pmatrix}, \; u_C^{1\ell} = \begin{pmatrix} 0_{2\times 3} \\ I_3 \end{pmatrix} \begin{pmatrix} F_x \\ F_z \\ \tau_\alpha \end{pmatrix}, \\ B_{1R_\alpha}^\ell = \begin{pmatrix} 0 & 0 & 0 \\ 0 & 0 & 0 \\ \cos\alpha & \sin\alpha & 0 \\ -\sin\alpha & \cos\alpha & 0 \\ 0 & -\frac{h}{2} & -1 \end{pmatrix}, \; u_{1R\alpha}^\ell = -\begin{pmatrix} I_3 & 0_3 \end{pmatrix} y_\partial^0, \\ B_{XZ}^i = \begin{pmatrix} 0 & 0 \\ 0 & 0 \\ 1 & 0 \\ 0 & 1 \\ (-1)^{i+1}\frac{L}{2}\cos\alpha & (-1)^i \frac{L}{2}\sin\alpha \end{pmatrix}, \\ u_{XZ}^i = -\begin{pmatrix} 0_2 & I_2 \end{pmatrix} y_\partial^i, \; B_d^\ell = \begin{pmatrix} 0 & 0 \\ 0 & 0 \\ 0 & 0 \\ 0 & 0 \\ 1 & \alpha \end{pmatrix}, \; u_d^\ell = -y_R, \end{gathered}$$

and $u_C^{1\ell}$ is included as a control input. With this the respective outputs can be calculated as

$$y_{R_\alpha}^\ell = {B_{R_\alpha}^\ell}^T \frac{\partial H_1^\ell}{\partial \mathrm{x}^1}, \tag{40}$$

$$y_{XZ}^i = {B_{XZ}^i}^T \frac{\partial H_1^\ell}{\partial \mathrm{x}^1}, \tag{41}$$

$$y_d^\ell = {B_d^\ell}^T \frac{\partial H_1^\ell}{\partial \mathrm{x}^1}. \tag{42}$$

This leads to a power exchange equal to

$$\dot{H}_1^\ell = (u_{R_\alpha}^\ell)^T y_{R_\alpha}^\ell + \sum_{i=1}^{2} (u_{XY}^i)^T y_{XY}^i + (u_d^\ell)^T y_d^\ell + (u_C^{1\ell})^T y_C^{1\ell}$$

3.4 Nacelle, Rotor and Blades

Finally, the second lumped system does not have any special interaction thus the energy of the system is given by the kinematic component. Thus the energy variables of this system are

$$\mathrm{x}^2 = \left(M_2^\ell v_a \Big|_{\xi^{F_0}=L_0} \; M_2^\ell v_T \Big|_{\xi^{F_0}=L_0} \; I_2^\ell r \Big|_{\xi^{F_0}=L_0} \right)^T, \tag{43}$$

and the Hamiltonian is given by

$$H_2^\ell = \frac{1}{2} (x^2)^T \mathcal{H}_2^\ell x^2, \tag{44}$$

where

$$\mathcal{H}_2^\ell = \mathrm{diag}\left(M_2^\ell \;\; M_2^\ell \;\; I_2^\ell \right)^{-1}. \tag{45}$$

By applying Hamilton's principle to (44) the dynamic equations for x^2 are obtained. It is possible to notice that the J matrix is 0_3 and the ODEs are

$$\dot{\mathrm{x}}^2 = B_{2R_\alpha}^\ell u_{2R_\alpha}^\ell + u_C^{2\ell}, \tag{46}$$

where

$$B_{2R_\alpha}^\ell = I_3, \quad u_{2R_\alpha}^\ell = -\left(0_3 \;\; I_3\right) y_\partial^0, \quad u_C^{2\ell} = \begin{pmatrix} F_a \\ F_T \\ \tau_\phi^\ell \end{pmatrix}. \tag{47}$$

Finally, the output can be expressed as

$$y_{2R_\alpha}^\ell = {B_{2R_\alpha}^\ell}^T \frac{\partial H_2^\ell}{\partial \mathrm{x}^2}, \tag{48}$$

This leads to the energy balance

$$\dot{H}_2^\ell = (u_{2R_\alpha}^\ell)^T y_{2R_\alpha}^\ell + (u_C^{2\ell})^T y_C^{2\ell}.$$

3.5 Gravity Interaction

To include the effects of gravity in the model the state space can be extended to add an energy variable representing the vertical displacement of a point. By adding the potential gravitational energy to the Hamiltonian, the skew-adjoint structure of the operator is preserved. This leads to an input mapping modulated by the angle of the floating platform α. One of the benefits of including the gravity effects through this method is when designing control strategies with energy based methodologies, such as energy shaping (Rodriguez et al., 2001), it is possible to attenuate disturbances caused by variations in the input mapping.

Table 1. Parameters for PDE described systems

String Parameters			
ρ_i	1630 kg/m^3	A_i	π2500e-6 m^2
E_i	10.4e9 Pa	G_i	1.39e9 Pa
L_i	750 m	z_i	$\pm$858 m
Beam Parameters			
ρ_0	7800 kg/m^3	A_0	$\pi(-2.08e\text{-}2\,\xi_1^{F_0} + 3.17)$ m^2
E_0	210e9 Pa	G_0	80e9 Pa
L_0	80 m	I_0	$\pi f(\xi_1^{F_0})$ $kg \cdot m^2$

$f(\xi_1^{F_0}) = -2.42e\text{-}6{\xi_1^{F_0}}^3 + 1.26e\text{-}3{\xi_1^{F_0}}^2 - 1.93e\text{-}1\xi_1^{F_0} + 9.91$

Table 2. Parameters for ODE described systems

Floating Platform			
L	108 m	M_1^ℓ	1.04e6 kg
h	24 m	I_1^ℓ	1.06e9 $kg \cdot m^2$
Nacelle, Rotor and Blades			
L_B	35 m	M_2^ℓ	67.4e3 kg
k_J	2.12e-1	I_2^ℓ	17.5e6 $kg \cdot m^2$

3.6 Damping incorporation

Internal damping is added to reflect the behavior of the real system and for numerical consistency. For this purpose, a Rayleigh dissipation function is considered, i.e.

$$R_d = \frac{1}{2} \int_{\Omega_1^{F_i}} (\dot{\zeta}^i)^T D_r \dot{\zeta}^i d\xi_1^{F_i}, \tag{49}$$

for $i = \{0, 1, 2\}$ leading to a damping term in the PDEs of the form

$$D^i = \left({P_1^i}^T \frac{\partial(\cdot)}{\partial \xi_1^{F_i}} - {P_0^i}^T \right) D_r \left(P_1^i \frac{\partial(\cdot)}{\partial \xi_1^{F_i}} + P_0^i \right) (\mathcal{H}_i \zeta^i), \tag{50}$$

where

$$D_r = \begin{pmatrix} D_q & 0 \\ 0 & 0 \end{pmatrix},$$

the damping matrix D_q being proportional to the stiffness matrix.

4. SIMULATION AND CONTROL PERSPECTIVES

In this section we discuss some numerical simulations and control perspectives.

4.1 Simulations

For the numerical implementation of the proposed model (and future control design using an early lumping approach), a structure preserving spatial discretisation scheme is required. In this work, a variation of the finite-difference discretisation scheme presented in Trenchant et al. (2018) is used to include the non-differentiated terms of the Timoshenko beam model, given by P_0^0 in (31). This spatial discretisation leads to a discrete system that keeps a port Hamiltonian structure and reflects the exchanges of energy with the system and with the environment. The parameters that have been used for the simulations can be found in Table 1 and Table 2. We also considered

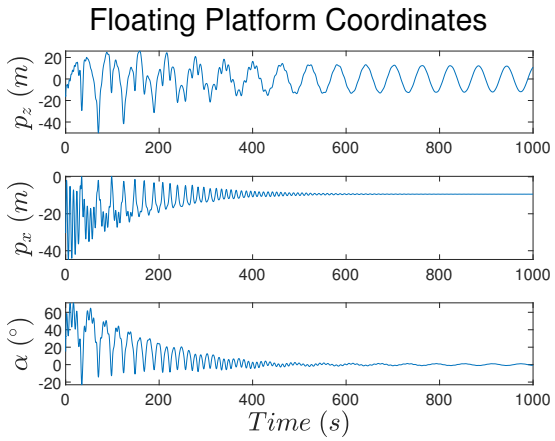

Fig. 2. Example of numerical simulation

$g = 9.81\,(m/s^2)$, $\rho_W = 1000\,(kg/m^3)$ and some damping matrices equal to 5% of the stiffness ones. With this set of parameters, stable simulations over 1000 seconds are obtained for a range of initial configurations with null inputs. An example of such simulation is given for initial values of $p_x = -30\,(m)$, $\alpha = \frac{\pi}{12}$ rad and $p_z = -15\,(m)$. Every momentum is set to 0, the strains of the strings are the constant spatial derivatives obtained from dividing the difference between (4) and (3) by L_i, and finally, the strains of the beam system have every spatial derivative equal to 0. In Figure 2 it is possible to see that the vertical position and the angle converge to an equilibrium in about 400 seconds, while the horizontal position converges with a slower rate. These convergence rates could be influenced by the water-structure interactions, which do not include the viscous damping of the water or the added mass effect.

4.2 Control Perspectives

In this paper we have propose a modular approach for the modelling of a quite complex Floating Wind Turbine leading to a small set of PDEs and ODEs consistent with energy balances that should help to develop control strategies for disturbance rejection or vibration suppression. A key benefit of formulating the proposed model within a port-Hamiltonian (PH) framework is that the well-posedness of and control design of systems described by PDEs like (31) has already been studied (Jacob and Zwart, 2018; Macchelli et al., 2017). Even if the aerodynamics of the NRB system or the hydrodynamics of the floating platform are modelled with greater precision, these effects can be encapsulated by the external inputs, or the lumped systems can be replaced by energy-preserving distributed systems.

Another advantage of the FWT model proposed in this work is its modularity. This enables the incorporation of modular models for the nacelle, rotor and blade system that include more precise effects of the control inputs. In the same fashion, it also allows to include more precise actuators like moving inertias or smaller propellers to stabilise the platform. In both cases, the energy-preserving structure can be leveraged to prove stability of proposed control strategies.

5. CONCLUSION

In this paper, we have presented a port-Hamiltonian system for a floating wind turbine that includes a Timoshenko beam model with axial and transverse deformation for the wind generator tower model, two-dimensional string models for the mooring system and lumped systems for the top of the tower and the floating platform. The presented system has a power preserving structure and is passive, leading to convergent simulations through a discretisation strategy that preserves the energy balance. In future work, the control perspectives should be applied and prove the stability of the proposed system while implementing disturbance rejection and vibration reduction control strategies. Additionally, more complete models of the aerodynamics or hydrodynamics could coupled through the system's modularity to better capture the complex environment.

REFERENCES

Bakka, T., Karimi, H.R., and Christiansen, S. (2014). Linear parameter-varying modelling and control of an offshore wind turbine with constrained information. *IET Control Theory & Applications*, 8(1), 22–29. doi: 10.1049/iet-cta.2013.0480.

Cruz, J. and Atcheson, M. (2016). *Floating offshore wind energy: the next generation of wind energy*. Springer.

Golo, G., Talasila, V., van der Schaft, A., and Maschke, B. (2004). Hamiltonian discretization of boundary control systems. *Automatica*, 40(5), 757–771. doi: https://doi.org/10.1016/j.automatica.2003.12.017.

González Rodriguez, A., González Rodriguez, A., and Burgos Payán, M. (2007). Estimating wind turbines mechanical constants. *Renewable Energy and Power Quality Journal*, 1, 697–704. doi:10.24084/repqj05.361.

He, W., Xiang, W., He, X., and Li, G. (2020). Boundary vibration control of a floating wind turbine system with mooring lines. *Control Engineering Practice*, 101, 104423. doi:10.1016/j.conengprac.2020.104423.

Jacob, B. and Zwart, H. (2018). An operator theoretic approach to infinite-dimensional control systems. *GAMM-Mitteilungen*, 41(4), e201800010.

Lannes, D. (2017). On the Dynamics of Floating Structures. *Annals of PDE*, 3, 11. doi:10.1007/s40818-017-0029-5.

Le Gorrec, Y., Zwart, H., and Maschke, B. (2005). Dirac structures and boundary control systems associated with skew-symmetric differential operators. *SIAM Journal on Control and Optimization*, 44(5), 1864–1892. doi: 10.1137/040611677.

Li, X. and Gao, H. (2016). Load mitigation for a floating wind turbine via generalized h_∞ structural control. *IEEE Transactions on Industrial Electronics*, 63(1), 332–342. doi:10.1109/TIE.2015.2465894.

Macchelli, A., Le Gorrec, Y., Ramírez, H., and Zwart, H. (2017). On the synthesis of boundary control laws for distributed port-hamiltonian systems. *IEEE Transactions on Automatic Control*, 62(4), 1700–1713. doi: 10.1109/TAC.2016.2595263.

Maschke, B. and van der Schaft, A. (2000). Port controlled hamiltonian representation of distributed parameter systems. *IFAC Proceedings Volumes*, 33(2), 27–37. doi:/10.1016/S1474-6670(17)35543-X. IFAC Workshop

on Lagrangian and Hamiltonian Methods for Nonlinear Control, Princeton, NJ, USA, 16-18 March 2000.

Ponce, C., Wu, Y., Le Gorrec, Y., and Ramirez, H. (2024). A systematic methodology for port-Hamiltonian modeling of multidimensional flexible linear mechanical systems. *Applied Mathematical Modelling*, 134, 434–451. doi:10.1016/j.apm.2024.05.040.

Robertson, A., Jonkman, J., Vorpahl, F., Popko, W., Qvist, J., Frøyd, L., Chen, X., Azcona, J., Uzunoglu, E., Guedes Soares, C., Luan, C., Yutong, H., Pengcheng, F., Yde, A., Larsen, T., Nichols, J., Buils, R., Lei, L., Nygaard, T.A., Manolas, D., Heege, A., Vatne, S.R., Ormberg, H., Duarte, T., Godreau, C., Hansen, H.F., Nielsen, A.W., Riber, H., Le Cunff, C., Beyer, F., Yamaguchi, A., Jung, K.J., Shin, H., Shi, W., Park, H., Alves, M., and Guérinel, M. (2014). Offshore code comparison collaboration continuation within iea wind task 30: Phase ii results regarding a floating semisubmersible wind system. volume Volume 9B: Ocean Renewable Energy of *International Conference on Offshore Mechanics and Arctic Engineering*, V09BT09A012. doi:10.1115/OMAE2014-24040.

Rodriguez, H., van der Schaft, A., and Ortega, R. (2001). On stabilization of nonlinear distributed parameter port-controlled Hamiltonian systems via energy shaping. In *Proceedings of the 40th IEEE Conference on Decision and Control (Cat. No.01CH37228)*, volume 1, 131–136. IEEE, Orlando, FL, USA. doi:10.1109/CDC.2001.980086.

Salic, T., Charpentier, J.F., Benbouzid, M., and Le Boulluec, M. (2019). Control strategies for floating offshore wind turbine: Challenges and trends. *Electronics*, 8(10), 1185 (14p.). doi:10.3390/electronics8101185.

Trenchant, V., Ramirez, H., Le Gorrec, Y., and Kotyczka, P. (2018). Finite differences on staggered grids preserving the port-hamiltonian structure with application to an acoustic duct. *Journal of Computational Physics*, 373, 673–697. doi:10.1016/j.jcp.2018.06.051.

Appendix A. ARCHIMEDES FORCES AND TORQUES